

RESEARCH

Open Access



Post-peak Behaviour of Composite Column Using a Ductile Lightweight Aggregate Concrete

Mohammad Reza Hamidian¹ and Payam Shafigh^{2*}

Abstract

Oil palm shell (OPS) concrete filled steel tube (CFT) columns are acknowledged to be a new type of sustainable composite column. In this type of column, the conventional coarse aggregate was partially replaced with OPS lightweight aggregate to provide a green composite column. This type of CFT column showed higher energy absorption and flexibility compared to CFT columns with normal weight concrete. This research studied the effect of the strength of OPS concrete on the axial compressive behaviour of CFT columns for two grades of OPS concretes. The behaviour was comparable to that of CFT columns with two grades of normal concrete. The results showed that the CFT columns with OPS concrete achieved a new post-peak behaviour. The experimental results of the axial compressive load were compared with the estimation of two international standards. EC4-1994 and ACI318-14 showed a reliable and conservative estimation of the axial load capacity of CFT columns, respectively.

Keywords: composite column, post-peak behaviour, ductile lightweight aggregate, CFT column, oil palm shell lightweight concrete, agricultural waste material

1 Introduction

Concrete filled steel tube (CFT) columns have been widely used in the construction industry because of their superior structural behaviour, such as high strength and ductility (Abed et al. 2013; Matsumoto et al. 2012). In addition, fast construction and cost savings for the framework have led to this composite being used in different structures, such as high-rise buildings (Matsumoto et al. 2012), bridges (Chacón et al. 2013; Li et al. 2016) and piles (Roeder and Lehman, 2012). Due to the composite action in CFT columns, the mechanical properties of both the concrete core and the steel tube significantly improved. This is attributed to two main reasons: (1) the concrete core provides lateral support for the steel tube

and delays the local buckling. (2) Surrounding the concrete core with a steel tube increases its triaxial stress, and, consequently, the strength and ductility of the concrete core improve (Shams and Saadeghvaziri, 1999). Therefore, a structure made of CFT columns has better performance compared to steel and reinforced concrete (RC) structures, especially under seismic and dynamic loads (Han et al. 2014). For instance, in the Hansin-Awaji earthquake in Japan in 1995, the steel structures and RC structures showed heavy damage, whereas the CFT structures avoided collapse (Xiamuxi and Hasegawa 2012).

Various studies have shown the advantages of CFT columns. In 1957, Klöppel and Goder carried out collapse load tests on CFT columns and proposed a design formula for CFTs (Gourley et al. 2008). Gardner and Jacobson (1967) attempted to predict the ultimate load of CFT columns. Furlong (1967 and 1968) investigated the behaviour of CFT columns in detail and pointed out the properties of CFTs. He presented design graphs and

*Correspondence: pshafigh@gmail.com

² Associate Professor, Centre for Building, Construction & Tropical Architecture (BuCTA), Faculty of Built Environment, University of Malaya, 50603 Kuala Lumpur, Malaysia

Full list of author information is available at the end of the article
Journal information: ISSN 1976-0485 / eISSN 2234-1315

formulas for CFT columns. In 1970, Knowles and Park (1969 and 1970) investigated axially loaded CFT columns with a wide range of slenderness ratios. They presented the design equations to compute the ultimate compression strength of CFT columns.

Considering the importance of CFT columns investigations, many projects were carried out on Composite and Hybrid Structures from 1993 (Nishiyama and Morino 2002). In these researches, experimental studies consisting of centrally loaded stub columns, eccentrically loaded stub columns, beam-column connections, high-strength materials and large width-to-thickness (D/t) ratios of CFT columns were conducted (Nishiyama and Morino 2002). The research topics covered in the aforementioned investigations are summarized as follows:

- i. Structural mechanics including the stiffness, strength, post-local buckling behaviour, confinement effects, stress transfer mechanisms, and the ductility of columns, beam columns, and beam-column connections;
- ii. Construction efficiency including concrete compaction, mixture, casting method and construction time;
- iii. Fire resistance including strength under fire and the amount of fireproof material.
- iv. Structural planning, including applications for high-rise and large-span buildings, and cost performance.

The results of these investigations have contributed greatly to improving the design and construction methods of CFTs. According to the results of investigations (Amano et al. 1998; Fujimoto et al. 1997; Huang et al. 2002; Jialin 1996; Jiuru et al. 2004; Matsui 1994; Nishiyama and Morino 2002; Schneider et al. 2004; Xiao et al. 2003; Zeghiche and Chaoui 2005), the main advantages of CFT columns may be summarized as follows:

- i. The concrete core is under a three-dimensional stress condition due to the lateral confining pressure provided by the steel tube and diaphragms, and this lateral confining pressure contributes to an increase in the compressive strength and ductility of the concrete core.
- ii. The steel tube prevents the concrete from peeling off and contributes to a smaller degradation in strength. Meanwhile, the drying shrinkage and creep of the concrete are much smaller than that for ordinary RC.
- iii. CFT enables high-strength steel and concrete to be utilized effectively, and, hence, the size of the cross section is reduced.

- iv. Fire resistance is improved as far as the thermal capacity of the filled concrete is concerned; hence, the fireproof material can be reduced or omitted.
- v. A concrete mould is unnecessary; hence, the CFT possesses excellent workability, such as saving labour and shortening the time for the works. Therefore, better economic performance is obtained with CFT structures compared to other types of structures.

2 Analysis of Previous Studies

The behaviour of CFT columns is a function of the compressive strength of the concrete core and yield strength of the steel tube. Han et al. (Han et al. 2010;) introduced a factor, namely, the confinement factor (ξ), to predict the post-peak behaviour of a CFT column. It can be calculated using Eq. 1:

$$\xi = \frac{A_{st}f_{yt}}{A_c f_{ck}}, \quad (1)$$

where A_c , A_{st} , f_{yt} and f_{ck} are cross-sectional area of concrete core, cross-sectional area of steel tube, yield stress of steel tube and characteristic concrete strength, respectively.

Figure 1 represents Eq. 1 for different confinement factors (Han et al. 2005). As can be seen in this figure, CFT columns with different confinement factors exhibit the same behaviour at the pre-peak stage. While, in the post-peak stage, a CFT column could demonstrate one of three types of behaviour—strain hardening, strain softening or elastic-perfectly plastic if $\xi > 1.1$, $\xi < 1.1$ and $\xi = 1.1$, respectively. The investigation and prediction of the post-peak behaviour of CFT columns are important, because it shows the energy absorption and failure mode of the columns. Researchers have shown that the strength of concrete has a significant effect on the post-peak

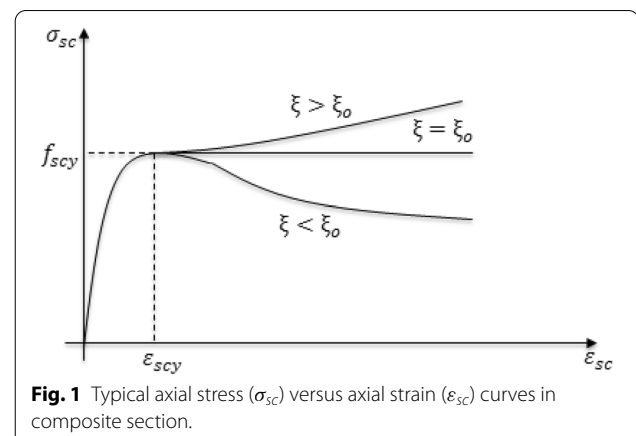


Fig. 1 Typical axial stress (σ_{sc}) versus axial strain (ϵ_{sc}) curves in composite section.

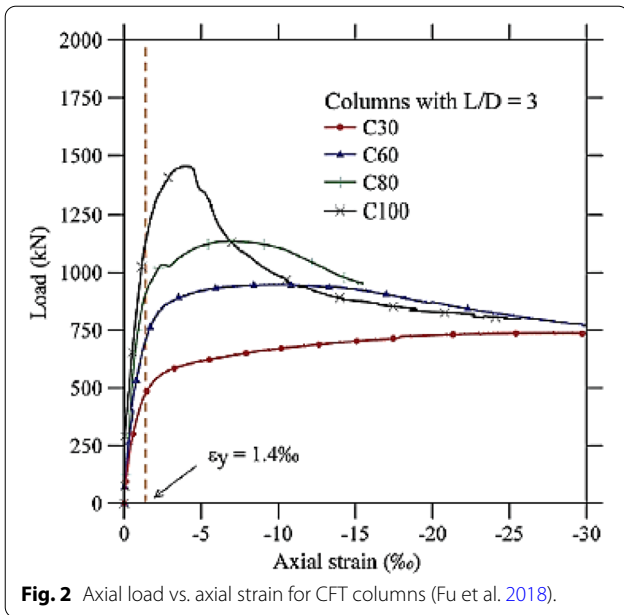


Fig. 2 Axial load vs. axial strain for CFT columns (Fu et al. 2018).

behaviour of CFT columns, and, consequently, the post-peak behaviour has a considerable effect on the structural properties of composite columns.

de Oliveira et al. (2009) studied the effect of the compressive strength of concrete on the post-peak behaviour of CFT columns. They investigated the behaviour of a series of CFT columns with the same steel tube and different grades of concrete under axial load. Figure 2 shows the axial load versus the axial strain curves of four groups of CFT columns with concrete grades 30, 60, 80 and 100. As can be seen in this figure, the increase in the compressive strength of concrete improved the ultimate load capacity of the column. However, the post-peak behaviour of CFT columns was significantly different. CFT columns with a lower grade of concrete showed strain-hardening behaviour, while those with a higher compressive strength showed strain-softening behaviour. The softening behaviour of CFT columns results in a load drop after peak load. As can be seen in Fig. 2, a CFT column with higher concrete compressive strength has a higher load drop at the softening stage. Figure 3 shows the load drop definition for CFT columns. The percentage of load drop has significant effect on the post-peak behaviour, energy absorption and overall structural performance of CFT columns.

Many researches have been conducted on the effect of the material properties on the behaviour of CFT columns. In these studies, different conditions for the steel tube and concrete core were considered. Figure 4 shows the relationship between the confinement factor (ξ) and the load drop percentage (LD %) of CFT columns based on 36 different CFT specimens reported by Han et al.

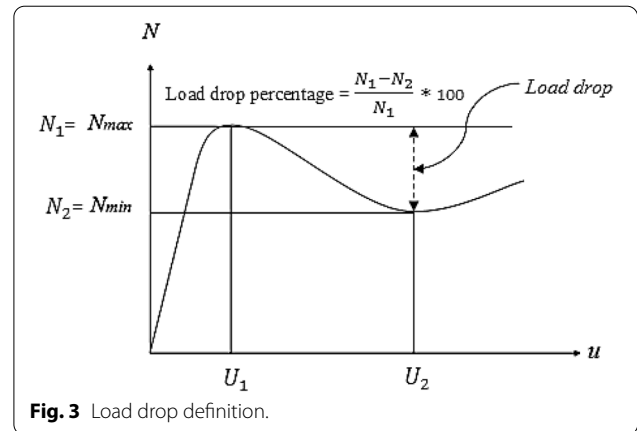


Fig. 3 Load drop definition.

(Han et al. 2005), Yu et al. (Yu et al. 2007), de Oliveira et al. (de Oliveira et al. 2009), and Xue et al. (Xue et al. 2012). As can be seen in this figure, the relation is linear with a strong correlation, and clearly shows that the increase in the compressive strength of the concrete core (and consequent reduction of ξ) results in a higher load drop at the softening stage.

It should be noted that for CFT columns with strain-softening behaviour that the circumstance of the load drop after peak load is another important factor to be considered in the analysis of CFT columns. As can be seen in Fig. 2, the drop in the load bearing capacity of the composite with grade 60 concrete was very gradual, while in the case of the grade 100 concrete, it was relatively sharp. This failure behaviour of CFT columns arising from changes in the compressive strength of the concrete is similar to the failure behaviour of the concrete core. The stress–strain curve of normal weight concrete shows that an increase in the compressive strength reduces the ultimate strain, and, consequently, concrete failure is due to brittle behaviour (Park and Paulay 1975).

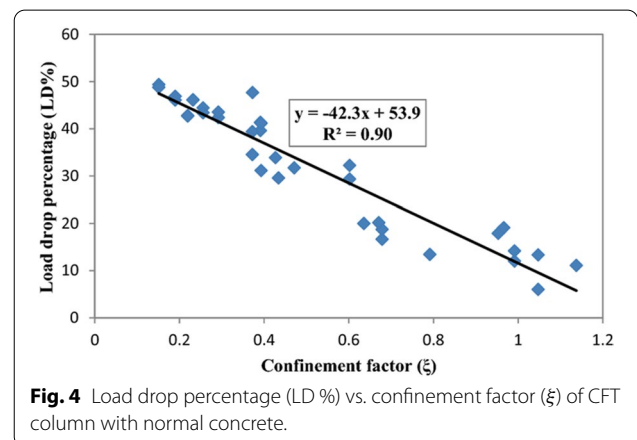


Fig. 4 Load drop percentage (LD %) vs. confinement factor (ξ) of CFT column with normal concrete.

In normal weight concrete, brittle behaviour occurs in high-strength grades, while in the case of lightweight aggregate concrete, this type of failure can be observed in the normal strength grades. This is because of the brittle nature of these groups of concrete (Cui et al. 2012; Hassanpour et al. 2012). Therefore, it is expected that if the concrete is a lightweight concrete of normal or high strength, the drop in the strength after the maximum load is sharp. However, one report (Shafigh et al. 2012) showed that among all the types of lightweight aggregate concrete, oil palm shell (OPS) lightweight concrete, for all grades of normal and high strength, has ductile behaviour.

In recent years, because of the high self-weight of normal concrete, investigations of CFT columns with lightweight concrete have been more attentive. Researchers have studied different features of CFT columns with different types of lightweight concrete such as bearing capacity (Zhang et al. 2019), effect of different types of aggregates (Yu et al. 2016), confinement effects (Hossain and Chu 2019; Raizamzamani et al. 2019) and effect of high-strength lightweight concrete (Salgar and Patil 2019). In addition, considering the benefits of lightweight concretes, using the lightweight concrete in the other types of CFT members such as composite beams have been more attention by researchers (Fu et al. 2016, 2018). OPS is a type of waste in the palm oil industry and has been used as a lightweight aggregate in concrete mixtures to produce structural lightweight concrete of normal and high strengths (Shafigh et al. 2010, Shafigh et al. 2011). Reports on the structural performance of OPS lightweight concrete in terms of flexural (Teo et al. 2006a), shear (Alengaram et al. 2011) and bond (Teo et al. 2007) behaviours show that this concrete has good potential to be used in constructing structural elements such as beams and slabs. This concrete was used in constructing a footbridge and a low-cost house as reported by Teo et al. (Teo et al. 2006b). Potential application of OPS lightweight concrete in CFT column was also reported (Hamidian et al. 2016b). This research focuses on the axial compressive behaviour of CFT columns made of OPS concrete of normal and high strengths. The effect of OPS concrete grade on the pre- and post-peak behaviours of CFT columns was studied, and the results were compared with normal concrete filled steel tube (NCFT) columns.

3 Experimental Programme

In this study, the axial behaviour of CFT columns with different grades of OPS concrete is considered. In addition, CFT columns with two grades of normal weight concrete were constructed and tested. Testing on CFT column with normal weight concrete was necessary to

verify the testing procedure and the test results based on the general behaviour of CFT columns; as shown in Fig. 4. The details of the materials used and the methods are as follows.

3.1 Materials Used

3.1.1 Concrete

Grades 30 and 40 OPS concrete, as normal and high-strength lightweight concretes, respectively, were used in this study. However, in the case of normal weight concrete, grades 40 and 55 were used as normal and high strengths. The mix proportions, slump and compressive strength test results at the time of testing the CFT columns are provided in Table 1.

It should be noted that for making grades 30 and 40 OPS concretes, approximately 75% of normal coarse aggregates (Granite) were replaced with OPS coarse lightweight aggregates in two different concrete mixtures. The method of mix proportioning was based on the recommendation reported by Shafigh et al. (2011b). The used coarse OPS aggregates had a specific gravity, abrasion value, crushing value, impact value, 24 h water absorption and maximum grain size of 1.19, 5.7%, 0.2%, 5.5%, 20.5% and 9.5 mm, respectively.

3.1.2 Steel

All the steel tube samples were cut to the same length of 400 mm from a hollow steel tube section of 6-m in length. Therefore, the specification for the steel tubes of the CFT columns is the same for all samples, and, hence, the results indicate the effect of the concrete type and strength on the behaviour of the composite columns. The outside diameter of the 3 mm thick steel tube was 140 mm. Based on the coupon test, using a 100 kN Instron tensile test machine, the yield stress of the steel tube was 355 kN.

Studies on the CFT column are usually in two groups of short and long columns. To investigate parameters such as the maximum load capacity, load-displacement behaviour, pre- and post-peak behaviours, the failure mode of concrete and local buckling of steel tube, short columns are used. However, to investigate the effect of overall buckling on the behavior of the CFT columns, long columns are used in studies. Therefore, in this investigation, a short column was studied.

3.2 Specimens

Based on the type of concrete, the specimens were divided into two groups: normal weight concrete filled steel tube (NCFT) and lightweight OPS concrete filled steel tube (LCFT). To ensure the accuracy of the experimental test results, for each type and grade of concrete,

Table 1 Mix proportions of normal and lightweight concretes.

Type of concrete	Concrete grade	Cement (kg)	Fly ash (kg)	Water (kg)	SP (%)	Coarse aggregate (kg)		Limestone powder (kg)	Sand (kg)	Slump (mm)	Density (Kg/m ³)	Compression strength (MPa)
						Granite	OPS					
NC	G40	400	0	200	0.5	980	0	0	855	200	2422	41.6
	G55	460	0	190	0.8	990	0	0	810	190	2458	55.2
LC	G30	480	0	173	1.0	222	305	0	805	125	1970	31.2
	G40	550	50	198	1.0	191	271	114	648	210	2008	40.9

two similar specimens were made and tested. Table 2 shows the details of the CFT specimens.

Concrete casting inside the steel tubes was conducted in three layers with each layer being compacted manually. Standard concrete cylinders (150 × 300 mm) were prepared from the same concrete batch that was used for CFT specimens. The standard cylinders were tested on the same day of testing as the CFT specimens. Based on the experimental testing of the CFT specimens, it was found that the surface texture of both ends of the CFT column has a considerable effect on the test results. Therefore, to achieve a smooth surface at both ends of the CFT specimens, all the specimens were capped with a high-strength mortar at both ends after 28 days of concrete curing. Figure 5 shows the fabrication steps of the specimens.

3.3 Test setup and instrumentation

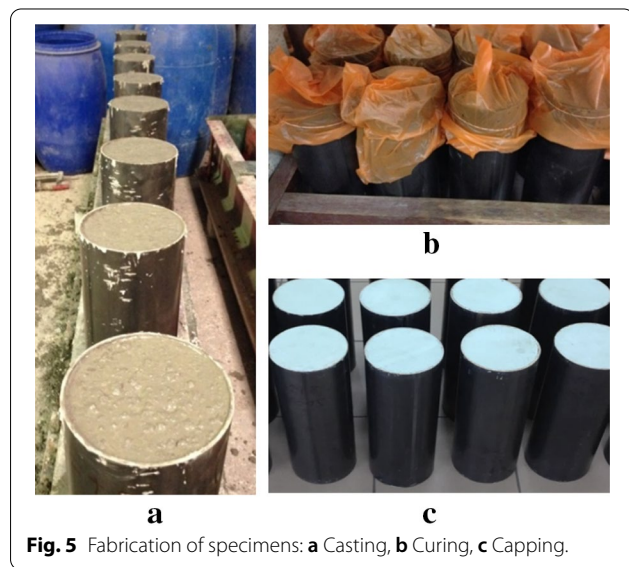
All the tests were conducted at the Construction Research Institute of Malaysia (CREAM). A Universal Testing Machine with 2000 kN capacity was used to conduct the experimental tests. Two LVDTs were used to measure the axial deformation of the specimens. Figure 6 demonstrates the test setup and the instrumentation used for the specimens. In this research, a mixed pattern of loading was used to perform the experimental tests. Loading pattern consists a monotonic axial loading at an initial rate of 75 kN/min, until the applied load reached 70% of the predicted maximum load. After that, the rate was changed to a displacement pattern of 0.6 mm/min until the end of the test (Hamidian, Jumaat, et al. 2016; Hamidian et al. 2016). To reduce the efficacy of looseness and unevenness as well as to avoid the stress concentration on the samples, all the samples were preloaded before the compression test with an axial load of 30 kN.

4 Test Results and Discussion

When an axial load is applied to CFT columns, the steel tube and the concrete core will both begin to deform longitudinally. In general, the behaviour of CFT columns can be divided into two main phases as before and after peak load. In the first phase, the behaviour of the CFT columns also consists of two stages: first, elastic behaviour, and, second, from the last elastic point to the peak load. The properties of the steel tube and the concrete core have an essential effect on the behaviour of CFT columns. In the elastic stage, CFT columns show almost the same behaviour for different types of materials. However, the behaviour of CFT columns in the second stage is more influenced by the properties of concrete (Hamidian et al. 2016). With the increase in axial load and after the second stage of the first phase, begins the second phase of the behaviour. Some of the most important

Table 2 Details of specimens.

Group	Concrete type	Concrete grade	Specimen label
1	Normal weight concrete	40	NCFT40-1
			NCFT40-2
		55	NCFT55-1
			NCFT55-2
2	Lightweight Oil palm shell concrete	30	LCFT30-1
			LCFT30-2
		40	LCFT40-1
			LCFT40-2

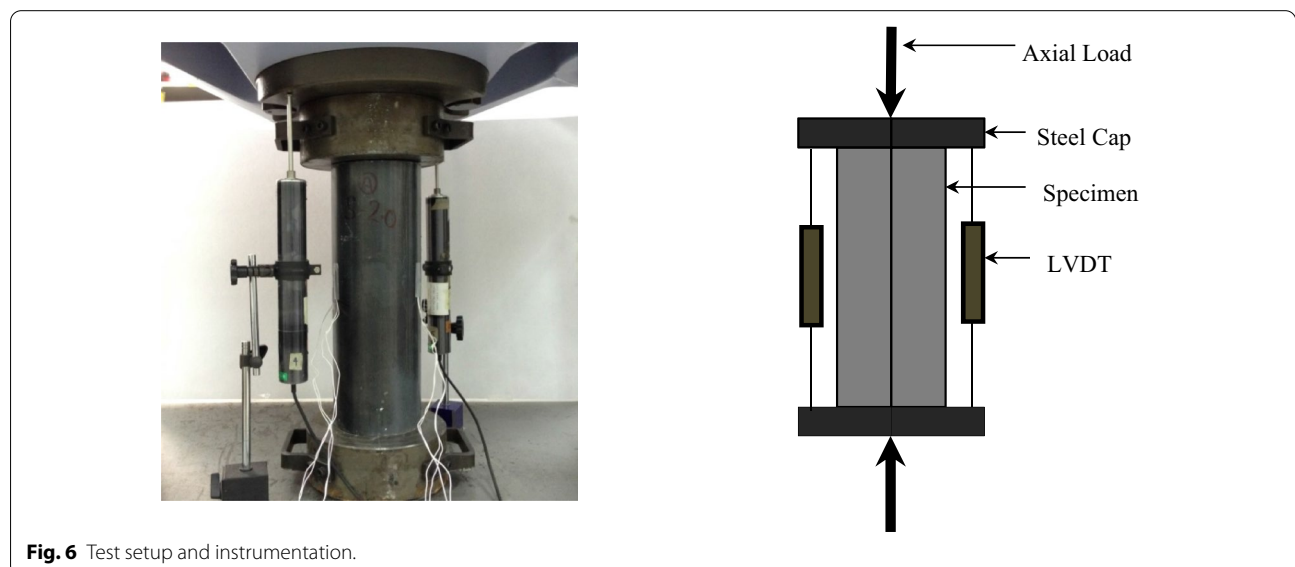


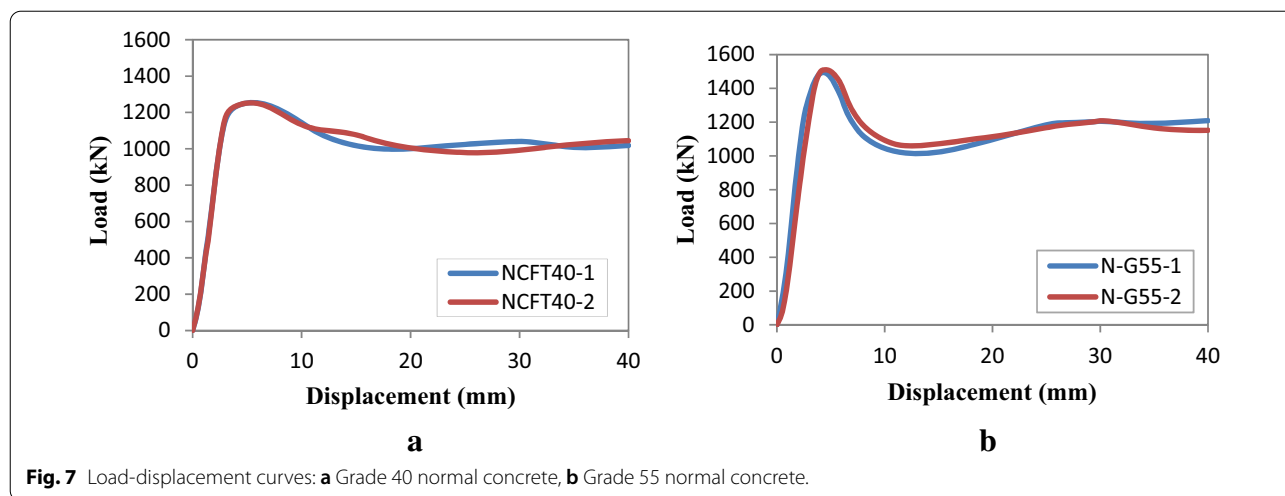
properties of the CFT columns such as ductility and the energy absorption capacity are depended on the post-peak behaviour of CFT columns. In the second phase, the properties of concrete have a considerable effect on the behaviour of CFT columns (Hamidian et al. 2016). To study the effect of concrete properties on the post-peak behaviour of the CFT column, two types of concrete as normal and OPS concrete were used and the results have been discussed in detail.

4.1 Axial Load Behaviour of CFT Column with Normal Weight Concrete

The load–displacement curves of the CFT specimens with grades 40 and 55 normal concrete are shown in Fig. 7. For each grade, two specimens with the same specification were tested. As can be seen in this figure, the load–displacement curves for the two specimens were almost the same, thereby demonstrating the accuracy of the sample preparation and testing. Due to the close results of the load–displacement for each grade of concrete, a mean value curve could be derived for each grade of concrete. Figure 8 shows the mean value curves for two grades of normal concrete.

From Fig. 8, it can be observed that the ascending part of the load–displacement curve of the CFT column for each grade of concrete increased linearly. This linear increase was exactly the same for both grades up to about 1200 kN. However, as expected, the length of the linear portion for the CFT column with greater strength was slightly longer. After the peak load, the load capacity was reduced for both concrete grades. The reduction for grade 40 was from 1253 kN to 999 kN, and for grade 55 it





was from 1501 kN to 1037 kN, thereby showing that the load capacity reduced by 20.3% and 30.9% for grade 40 and 55, respectively. After these reductions, both types of CFT column showed strain hardening behaviour. The strain hardening for grade 40 showed a slight increase in strength, while for the CFT column with grade 55, the increment in strength was more significant.

Figure 9 shows the relationship between the confined factor and the load drop percentage for CFT specimens with normal concrete. As can be seen in this figure, the increase in the confinement factor (resulting from a reduction in the compressive strength of the concrete) reduced the load drop percentage. This behaviour follows the general relation between the confinement factor and the load drop percentage; as shown in Fig. 10. This figure shows that the result for four CFT specimens with normal concrete was very close to the general trend line. Therefore, considering the new data from this study together with previous data, a new equation with higher accuracy and validity could be derived. Hence, based on the available data from the literature and the experimental test results of this study the following equation can be proposed to predict the load drop percentage of CFT columns constructed with normal weight concrete:

$$LD\% = -42.2\xi + 54, \tag{2}$$

where LD and ξ are load drop and confinement factor, respectively.

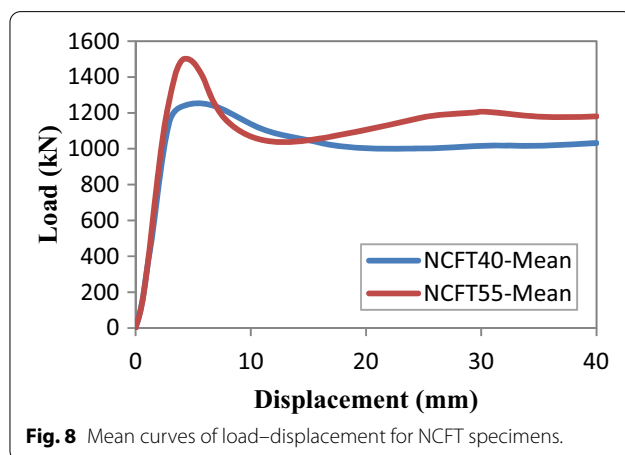
4.2 Axial Load Behaviour of CFT Columns with OPS Lightweight Concrete

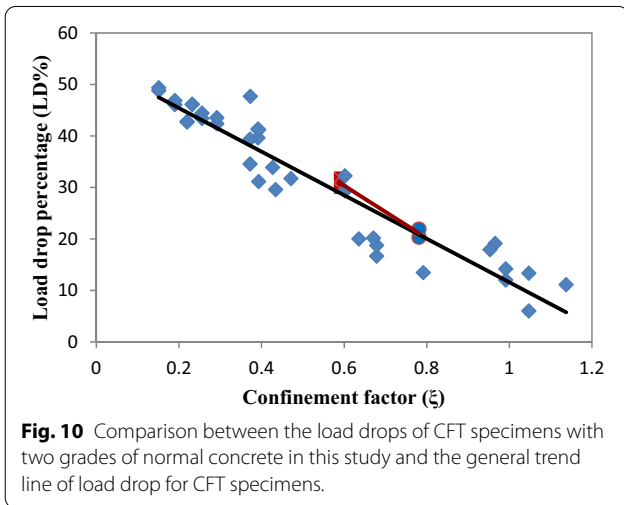
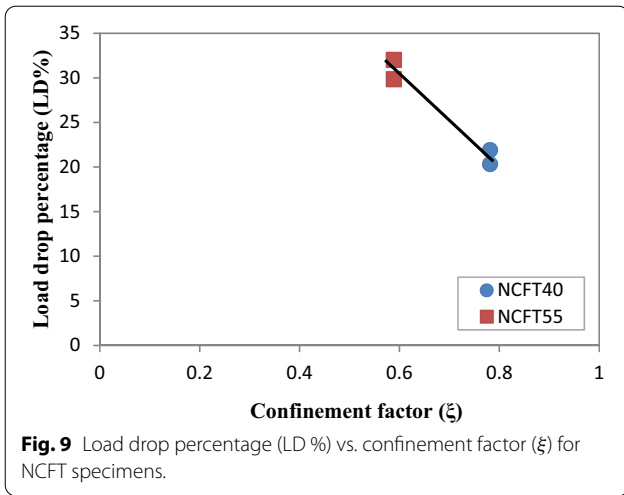
4.2.1 Pre-peak Behaviour

Figure 11 shows the axial load–displacement curves for the CFT columns constructed with grades 30 and 40 OPS lightweight concrete. For each grade of concrete, two similar specimens were prepared and tested. As can

be seen in these figures, the two curves for each type of CFT specimen were similar. Therefore, a mean curve was plotted to compare the axial load behaviour of CFT columns with grades 30 and 40 OPS concrete; the curves are shown in Fig. 12. Similar to the CFT column with normal weight concrete, the ascending portion of these curves for grades 30 and 40 OPS concrete was the same up to about 70% of the maximum load of LCFT40. The ascending portion of the CFT column was longer, and, consequently, the maximum load for LCFT40 was higher than that for LCFT30.

Generally, the linear part of the ascending portion of the CFT column with OPS lightweight concrete was similar to the CFT column with normal concrete. However, a comparison between LCFT40 and NCFT40 shows that the length of the curve from the last point of the linear part to the maximum point was longer for LCFT40. This shows that the CFT column containing OPS concrete has obvious plastic behaviour before the peak load, which





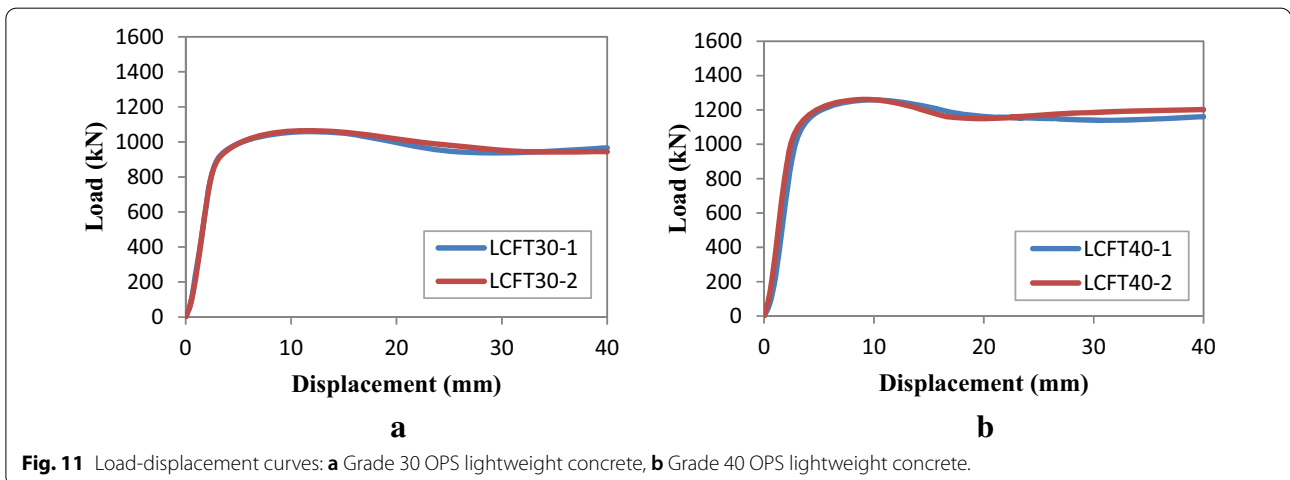
means that the CFT column containing OPS concrete with normal or high strength showed ductile behaviour at the pre-peak stage. For instance, it was observed that for the same concrete grade of 40 the U1 for the CFT column with OPS concrete was about 70% more than for the CFT column with normal weight concrete.

4.2.2 Post-peak Behaviour

As can be seen in Fig. 12, for both LCFT30 and LCFT40, the load was gradually reduced after maximum load. The load reduction continued up to about 90% of the maximum load. Figure 13 shows the maximum and minimum loads and corresponding displacements for all the CFT specimens in this study.

In this figure, the slope of each line shows the intensity of the load reduction after the peak load. There is not much difference between the line slopes for the CFT specimens with OPS concrete. However, there was a significant difference between the two types of CFT specimens with normal weight concrete. It can also be observed that the line for NCFT40 was steeper than the line for LCFT40. This shows that the CFT column with OPS concrete was more ductile compared to the CFT column with normal weight concrete at the same compressive strength. The load drop percentage of the CFT columns with grade 30 and 40 OPS concrete was 11.3% and 8.4%, respectively. While based on the proposed equation Eq. (2), the load drop percentage for the CFT column with grade 30 and 40 normal weight concrete should be 10% and 20.5%, respectively.

This shows that the load drop of the CFT column with OPS concrete exhibited a different trend compared to the CFT column with normal weight concrete. This difference in the post-peak stage can be observed in Fig. 14. As can be seen in this figure, the load drop in the CFT column with OPS concrete did not follow the load drop trend of the CFT column with normal weight



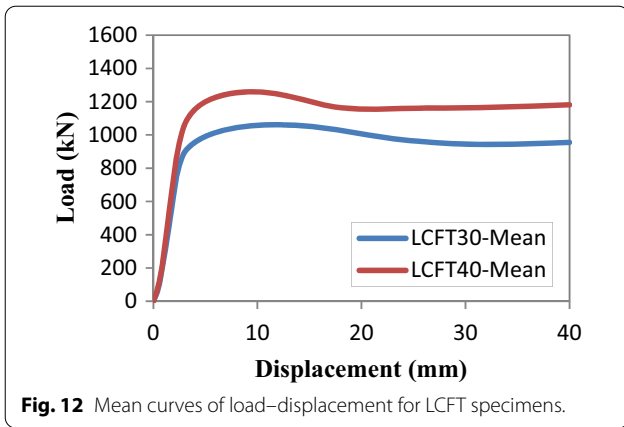


Fig. 12 Mean curves of load–displacement for LCFT specimens.

concrete. This means that the load drop percentage in the LCFT specimens shows almost the same value for different grades of concrete, while the higher grade of concrete results in a higher load drop percentage for the NCFT columns.

4.3 Failure Mechanism of Specimens

4.3.1 CFT Column with Normal Concrete

The failure mechanism of a CFT column with normal concrete was previously investigated and explained (Fam et al. 2004; Hamidian et al. 2016). Under an axial compression load, a major diagonal crack formed in the concrete core of the CFT column which was associated with a drop in the load–displacement curve. After cracking, the confinement effects due to the steel tube made a triaxial condition for the concrete core and increased the friction stress in the cracked surfaces. This process established the main mechanism for the resistance of the CFT columns against the applied axial load (de Oliveira et al. 2009; Fam et al. 2004). The increase in the friction stress of the cracked surfaces in the concrete results in better performance of the CFT column after cracking. For instance, a thicker steel tube can apply a greater confinement effect on the concrete core, and, consequently, increase the friction stress on the cracked surfaces.

4.3.2 CFT Column with OPS Concrete

The CFT column with OPS showed different behaviour compared to the CFT column with normal concrete, especially after the peak load. Hamidian et al. (2016) have shown that for the same grades of concrete, CFT columns with OPS concrete exhibit better post-peak behaviour compared to CFT columns with normal concrete. The better performance of CFT columns with OPS concrete is attributed to the different action in the cracked surfaces after diagonal cracking. Indeed, the two types of CFT column presented different failure mechanisms.

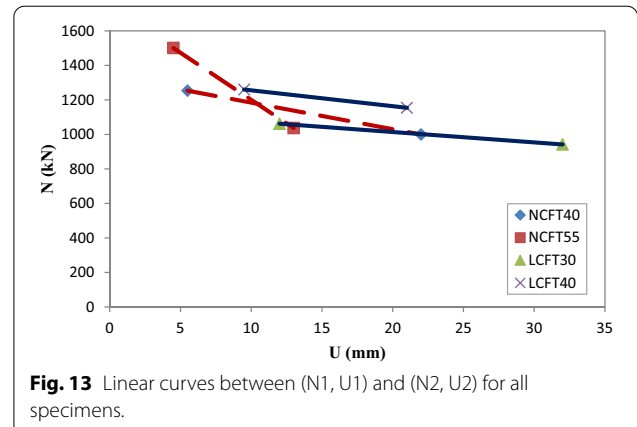


Fig. 13 Linear curves between (N1, U1) and (N2, U2) for all specimens.

Figure 15 shows the cracked surfaces for two types of normal and OPS concrete after the splitting tensile test. As can be seen in this figure, the surface texture of the granite concrete is relatively smooth, while for OPS concrete, it is very rough due to uncrushed OPS aggregates. The different conditions in the cracked surfaces created a different friction stress distribution and resulted in different behaviour for the CFT column with normal concrete to that of the CFT column with OPS concrete. The uncrushed OPS aggregate in the cracked surfaces created a higher friction force compared to the crushed granite aggregate that could slide much easier against each other. Therefore, in addition to the strength grade of concrete (de Oliveira et al. 2009), the characteristics of the crack surfaces affect the behaviour of CFT columns, especially in the post-peak stage.

As mentioned in the literature, concrete with a higher strength grade showed more brittle behaviour and caused a sharper drop in the CFT columns. As can be seen in Fig. 14, the CFT column with grade 55 normal concrete showed a much sharper drop ($U2=13$ cm) compared to that for grade 40 ($U2=22$ cm). In addition, the CFT

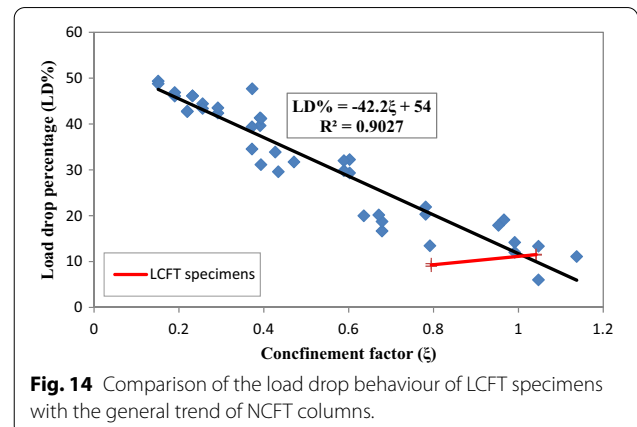


Fig. 14 Comparison of the load drop behaviour of LCFT specimens with the general trend of NCFT columns.

columns with OPS concrete showed a sharper drop for grade 40 concrete ($U_2=21$ cm) compared to those with grade 30 ($U_2=32$ cm). This means that CFT columns with OPS concrete follow the general rule for the concrete strength effect. However, there was a significant difference between the two types of CFT column in the load drop percentage. The CFT column with normal concrete exhibited a higher load drop percentage for grade 55 (LD % = 30.9%) compared to that for grade 40 (LD % = 20.3%). This means that the load drop for the CFT column with grade 55 concrete was 52% higher than that for grade 40.

However, the CFT column with OPS concrete showed almost the same load drop percentage for two grades of concrete—8.4% and 11.4% for grades 40 and 30, respectively. This showed a 7% difference between the load drop percentages for the two grades of OPS concrete. This difference when compared to CFT columns with normal concrete was not significant. The considerable difference in the load drop for the two types of CFT columns with normal and OPS concrete could be explained by the failure mechanism after the peak load.

After the diagonal crack, the friction forces between the two cracked surfaces caused an internal reaction against the applied loads. This could differ according to the condition of the cracked surfaces and result in the different post-peak behaviour for the different CFT columns.

Aggregate occupies most of the volume of the concrete mixture and significantly influences the properties of concrete (Kozul and Darwin 1997). Therefore, the

reaction of the aggregate has a major role in the behaviour of cracked surfaces. Figure 16 shows the schematic reaction of granite and OPS aggregate under applied shear force in the diagonal crack.

Because of the high brittleness, the failure of granite aggregate is associated with a sudden fracture that causes two separate broken surfaces (see Fig. 15a), while OPS aggregate shows highly flexible behaviour (Hamidian et al. 2016; Shafigh et al. 2012). OPS aggregate exhibits highly ductile behaviour with a significant deformation capacity under applied loads. An OPS grain is composed of high-strength fibres with high ductility. Therefore, OPS aggregate can show considerable deformation without a notable reduction in its energy absorption. Figure 16b and detail A show the schematic model for OPS aggregate with the flexible fibres under shear deformation due to shear stress.

The considerable similarity in the post-peak behaviour of two grades of OPS concrete, with almost the same load drop percentage, can be explained based on the ductile behaviour of OPS aggregate. Table 1 shows that the OPS content for the two grades of OPS concrete was almost the same. Therefore, considering that OPS aggregate plays a major role against the shear stresses in the diagonal crack, it could be expected that the failure mechanism of OPS concrete exhibits almost the same behaviour. Other characteristics of concrete, such as the compressive strength and mix components, can cause some differences in the final behaviour of grades 30 and 40 OPS concrete.

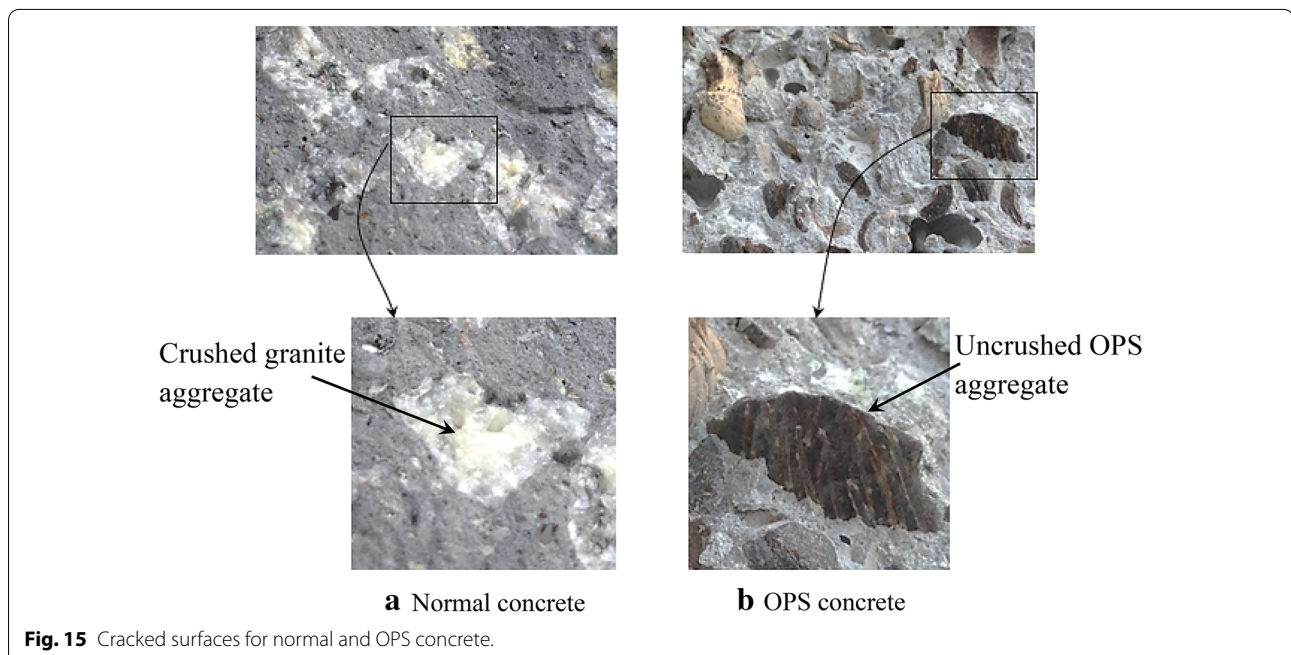


Fig. 15 Cracked surfaces for normal and OPS concrete.

Grade 40 CFT columns with OPS concrete showed an 8.4% load drop after peak load, while grade 30 showed an 11.4% load drop. This revealed that grade 40 exhibited a slightly lower load drop percentage compared to grade 30. This behaviour was significantly different to the known behaviour of CFT columns with normal concrete (see Figs. 2 and 4). This can be explained by the high capacity of OPS grains for deformation and their flexibility. In OPS concrete with higher compressive strength, more shear stresses can be transferred to the OPS aggregate before damage. Indeed, high-strength OPS concrete has better interaction between the concrete and OPS aggregate in the cracked surfaces.

4.3.3 Failure Mode of Specimens

Figure 17 shows the failure mode of specimens after testing. Figure 17a, b shows the cut samples of CFT columns with normal and OPS concrete, respectively. The diagonal cracks can be observed in these figures. As can be seen, the crack lines in the CFT columns with normal concrete are clearer than the CFT columns with OPS concrete. This can be explained by the better stress distribution in the CFT columns with OPS concrete, which is due to the high flexibility and ductile behaviour of OPS aggregate (Hamidian et al. 2016).

Figure 17c, d shows the CFT specimens after removing the loose crushed concrete for normal and OPS concretes, respectively. This figures show that, all the granite aggregate in the CFT column with normal concrete broke along the diagonal crack, while the OPS aggregates did not break. Separation of the broken pieces of normal concrete was easy, while for OPS concrete, it was not possible. This is because the uncrushed OPS grains act as a fibre and reinforce the concrete.

4.4 Ductile Behaviour of Specimens

Ductility behaviour of CFT specimens with different grades of normal and OPS concretes was investigated. The definition of displacement ductility that presented in Fig. 18 (Guler et al. 2013; Rakhshanimehr et al. 2014) was used to compare the ductile behaviour of specimens. Figure 18a, b shows the strain-hardening and strain-softening behaviour of specimens and their corresponding definitions of ductility, respectively. Two groups of the specimens showed completely different behaviour based on the definition of the ductility. Table 3 also shows the ductility index based on the condition of the specimens. As can be seen in this table, the behaviour of the samples in the OPS concrete group is much more ductile compared to the normal concrete group.

4.5 Comparison of Experimental Test Results and Standards

The load bearing capacity of the CFT columns from the experimental test results was compared with the predicted values from the codes of practice, EC4 (1994) and ACI 318-14 (2014). Based on EC4, the axial compressive strength of a CFT column can be calculated from the following equation:

$$N_{EC4} = \eta_a A_{st} f_{yt} + A_c f'_c \left(1 + \eta_c \frac{t}{D} \frac{f_{yt}}{f'_c} \right), \quad (3)$$

where η_a and η_c are factors related to the confinement of concrete, t and D are wall thickness of steel tube and diameter of steel tube.

For a pure axial loading on the column, the value for $\eta_a = \eta_{a0}$ and $\eta_c = \eta_{c0}$ can be calculated from Eqs. (3a) and (3b), respectively:

$$\eta_{a0} = 0.25 (3 + 2\bar{\lambda}) \quad (3a)$$

$$\eta_{c0} = 4.9 - 18.5\bar{\lambda} + 17\bar{\lambda}^2 \quad (3b)$$

$$\bar{\lambda} = \sqrt{\frac{N_{pl,Rk}}{N_{cr}}} \quad (3c)$$

$$N_{pl,Rk} = A_{st} f_{yt} + A_c f'_c \quad (3d)$$

$$N_{cr} = \frac{\pi^2 (EI)_{eff}}{l^2} \quad (3e)$$

$$(EI)_{eff} = E_a I_a + E_s I_s + K_e E_{cm} I_c \quad (K_e = 0.06), \quad (3f)$$

where $\bar{\lambda}$, $N_{pl,Rk}$ and N_{cr} are relative slenderness, characteristic value of the plastic resistance of the composite section to compressive normal force and elastic critical normal force, respectively. $(EI)_{eff}$, E_a , E_s and E_{cm} are effective flexural stiffness for calculation of relative slenderness, modulus of elasticity of steel tube, modulus of elasticity of steel bar and secant modulus of elasticity of concrete, respectively. I_a , I_s , I_c are second moment of area of the steel tube, second moment of area of the steel bar and second moment of area of the un-cracked concrete section, respectively.

ACI 318-14 provides the following equation to determine the axial capacity of CFT columns:

$$N_{ACI} = 0.85 A_c f'_c + A_{st} f_y \quad (4)$$

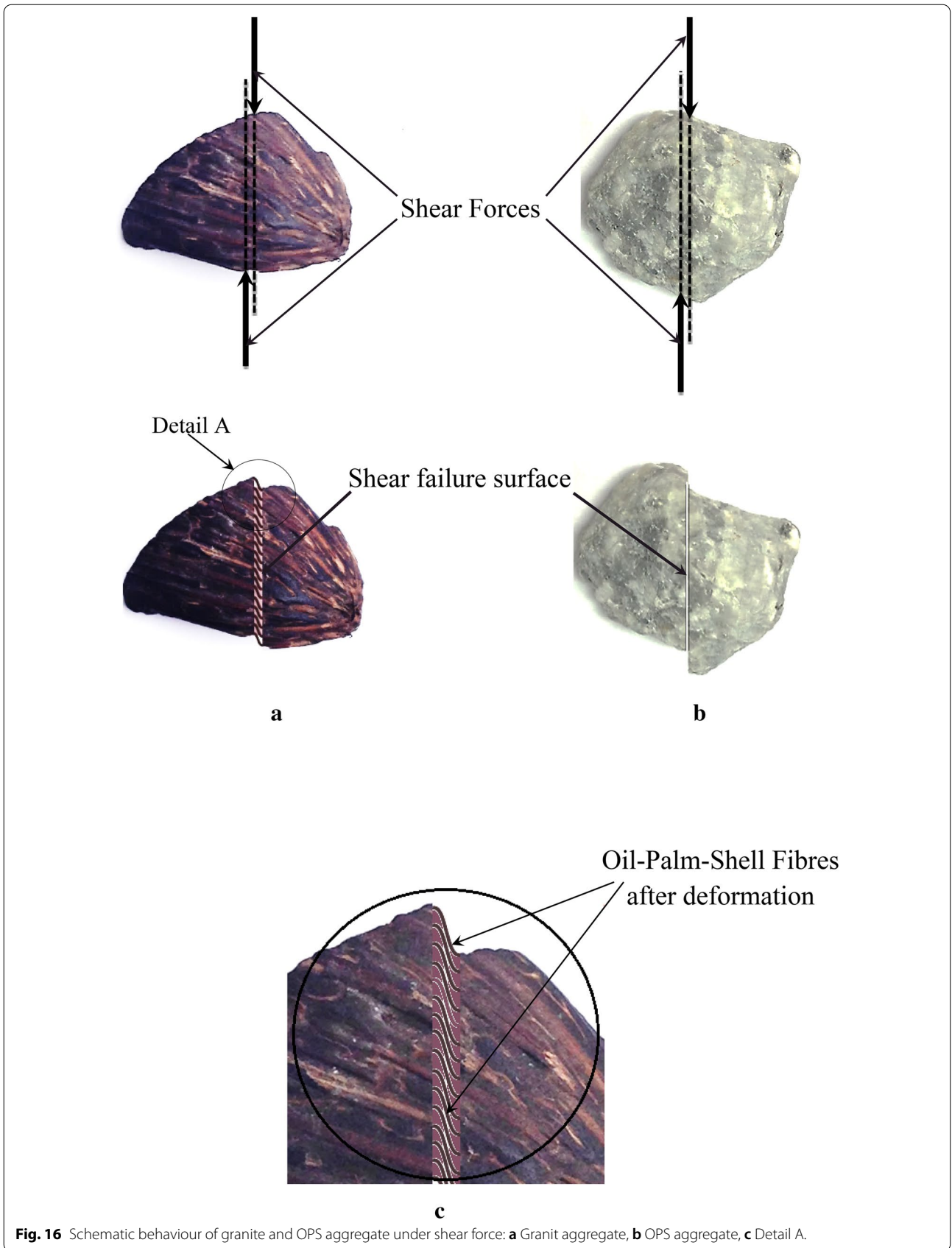


Fig. 16 Schematic behaviour of granite and OPS aggregate under shear force: **a** Granit aggregate, **b** OPS aggregate, **c** Detail A.

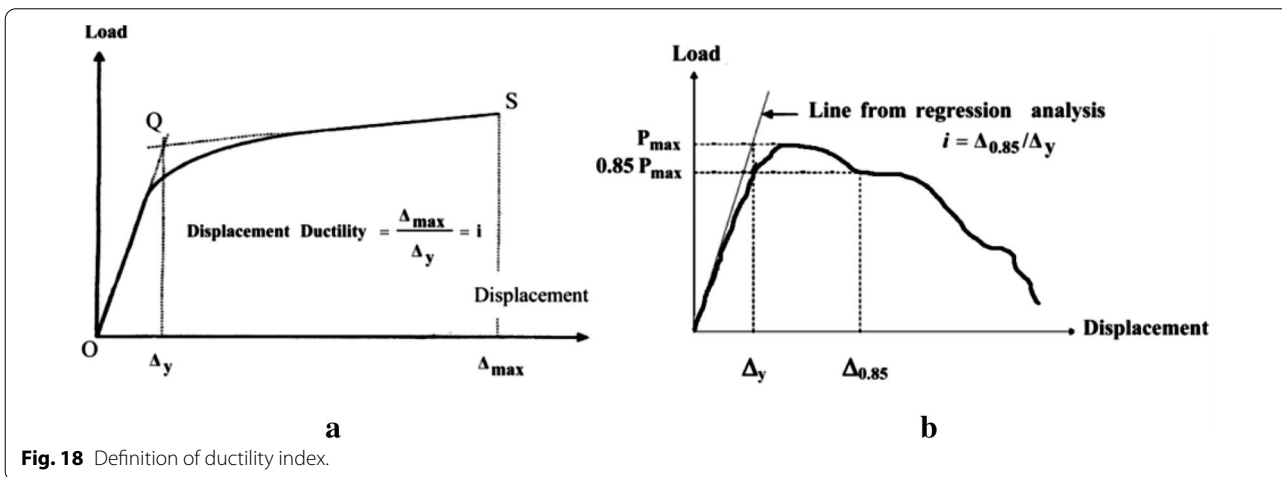
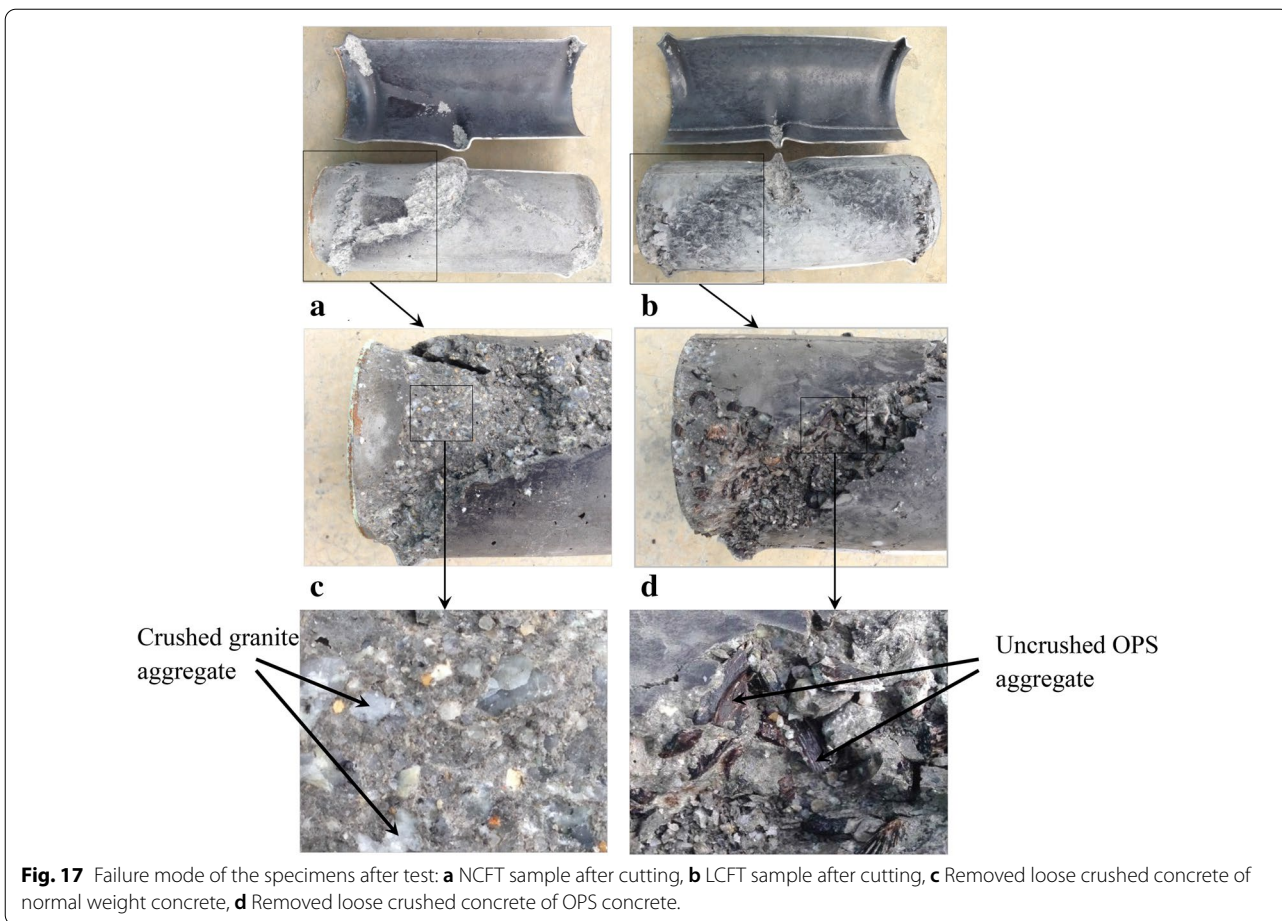


Table 4 summarises the results obtained from the experimental test and the two codes. This table shows a considerable difference between the predicted axial compressive strength for CFT columns with the EC4 and ACI standards. On average, the experimental test results

are 7% less than the predicted values from EC4 and 31% more than that for ACI 318-14. The axial capacity for the CFT columns predicted by EC4 is reliable, while it is conservative for ACI 318-14. The notable difference between the two codes is because EC4 considers the confinement

Table 3 Ductility index of specimens.

Specimen	Δ_y	$\Delta_{0.85} (\Delta_{Max})$	$\mu = \Delta_y / \Delta_{0.85} (\Delta_{Max})$
NCFT55	3.2	6.7	2.1
NCFT40	3.3	13.5	4.1
LCFT40	3.0	40	13.3
LCFT30	3.1	40	12.9

effect in the prediction model, whereas ACI 318-14 does not consider this effect. The reliable estimation of EC4 and the conservative prediction of ACI for CFT columns has been reported by other researchers (Giakoumelis and Lam 2004; Lu and Zhao 2010).

5 Conclusion

In the present study, eight CFT samples in four groups were tested. The effects of two grades of normal and OPS concrete were investigated on the behaviour of CFT columns. The following conclusions can be drawn from the results of this study.

1. CFT columns with OPS concrete have a new post-peak behaviour compared to conventional concrete. The load drop percentage for concrete grades 30 and 40 were similar.
2. Coarse aggregate plays a significant role in the post-peak behaviour of CFT columns. The strength and shear characteristics of coarse aggregate dominate the failure mechanism, and, consequently, the post-peak behaviour of CFT columns.
3. OPS aggregate shows highly ductile behaviour against the shear stress in the diagonal crack of the CFT columns compared to granite aggregate with brittle failure.
4. EC4-1994 and ACI 318-14 showed a reliable and conservative estimation of the axial capacity of CFT columns, respectively. On average, EC4 estimated 7% more and ACI 318-14 estimated 31% less than the experimental test results.

Abbreviations

A_c : Cross-sectional area of concrete core; A_g : Cross-sectional area of composite column; A_{st} : Cross-sectional area of steel tube; D : Diameter of steel tube; E_s : Modulus of elasticity of steel tube; E_{cm} : Secant modulus of elasticity of concrete; f_{yt} : Yield stress of steel tube; f'_c : Compressive strength of standard cylinder; f_{ck} : Characteristic concrete strength ($f_{ck} = 0.67 f_{cu}$); f_{cu} : Concrete cube strength; f_{sc} : The stress corresponding to the ultimate load of the composite sections; I_g : Second moment of area of the steel tube; I_c : Second moment of area of the un-cracked concrete section; I_s : Second moment of area of the

Table 4 Comparison of test results with EC4 and ACI 318-14.

Group	No.	Label	Nexp (kN)	Nexp/NEC4	Nexp/NACI
1	1	NCFT40-1	1252	0.93	1.31
	2	NCFT40-2	1252	0.93	1.31
2	3	NCFT55-1	1491	0.97	1.33
	4	NCFT55-2	1510	0.99	1.35
3	5	LCFT30-1	1058	0.88	1.27
	6	LCFT30-2	1065	0.88	1.28
4	7	LCFT40-1	1259	0.94	1.33
	8	LCFT40-2	1262	0.94	1.33
Average				0.93	1.31

steel bar; L : Length of specimen; N_1 : Maximum axial strength of specimen (peak load); N_2 : Minimum axial strength of specimen after load drop (lowest load); N_{exp} : Experimental ultimate strength; t : Wall thickness of steel tube; U_1 : Displacement corresponding to maximum axial load (N_1); U_2 : Displacement corresponding to minimum axial load after load drop (N_2); ϵ_{sc} : The strain corresponding to the ultimate load of the composite sections; ϵ_{sc} : Axial strain in composite section; σ^c : Axial stress in composite section; ξ : Confinement factor; $\Delta_{0.85}$: Displacement corresponding to 85% of the maximum load on the post-peak portion; Δ_y : First yield displacement; Δ_{Max} : Maximum displacement; μ : Ductility index.

Authors' information

Mohammad Reza Hamidian is an Assistant Professor in the Department of Civil Engineering at Islamic Azad University-Kerman Branch. Payam Shafigh is an Associate Professor in the Department of Architecture and Centre for Building, Construction & Tropical Architecture (BuCTA) at University of Malaya.

Authors' contributions

All authors equally contributed for this study. All authors read and approved the final manuscript.

Funding

Not applicable.

Availability of data and materials

All data generated or analysed in this research are included in this published article.

Competing interests

The authors declare that they have no competing interests.

Author details

¹ Assistant Professor, Department of Civil Engineering, Kerman Branch, Islamic Azad University, Kerman, Iran. ² Associate Professor, Centre for Building, Construction & Tropical Architecture (BuCTA), Faculty of Built Environment, University of Malaya, 50603 Kuala Lumpur, Malaysia.

Received: 30 January 2020 Accepted: 28 August 2020

Published online: 18 February 2021

References

- Abed, F., AlHamaydeh, M., & Abdalla, S. (2013). Experimental and numerical investigations of the compressive behavior of concrete filled steel tubes (CFSTs). *Journal of Constructional Steel Research*, 80, 429–439.
- ACI 318-14. Building Code Requirements for Structural Concrete (ACI 318-14) and Commentary. American Concrete Institute.

- Alengaram, U. J., Jumaat, M. Z., Mahmud, H., & Fayyadh, M. M. (2011). Shear behaviour of reinforced palm kernel shell concrete beams. *Construction and Building Materials*, 25, 2918–2927.
- Amano, M., Kasai, A., Usami, T., Ge, H., Okamoto, O., & Maeno, H. (1998). Experimental and analytical study on elasto-plastic behaviour of partially concrete-filled steel bridge piers. *Structural Engineering JSCE*, 44, 179–187.
- Chacón, R., Mirambell, E., & Real, E. (2013). Strength and ductility of concrete-filled tubular piers of integral bridges. *Engineering Structures*, 46, 234–246.
- Cui, H. Z., Lo, T. Y., Memon, S. A., Xing, F., & Shi, X. (2012). Analytical model for compressive strength, elastic modulus and peak strain of structural lightweight aggregate concrete. *Construction and Building Materials*, 36, 1036–1043.
- de Oliveira, W. L. A., De Nardin, S., et al. (2009). Influence of concrete strength and length/diameter on the axial capacity of CFT columns. *Journal of Constructional Steel Research*, 65, 2103–2110.
- Ec4 1994. Design of composite steel and concrete structures (EN 1994). European Committee for Standardization: British Standards Institution.
- Fam, A., Qie, F. S., & Rizkalla, S. (2004). Concrete-filled steel tubes subjected to axial compression and lateral cyclic loads. *Journal of Structural Engineering*, 130, 631–640.
- Fu, Z.-Q., Ji, B.-H., Zhu, W., & Ge, H.-B. (2016). Bending behaviour of lightweight aggregate concrete-filled steel tube spatial truss beam. *Journal of Central South University*, 23, 2110–2117.
- Fu, Z., Wang, Q., Wang, Y., & Ji, B. (2018). Bending performance of lightweight aggregate concrete-filled steel tube composite beam. *KSCCE Journal of Civil Engineering*, 22, 3894–3902.
- Fujimoto, T., Mukai, A., Nishiyama, I., et al. (1997). Axial compression behavior of concrete filled steel tubular stub columns using high strength materials. *Journal of Structural and Construction Engineering (Transactions of AIJ)*, 62(498), 161–168. <https://doi.org/10.3130/aijs.62.161>.
- Furlong, R. W. (1967). Strength of steel-encased concrete beam columns. *Journal of the Structural Division*, 93, 113–124.
- Furlong, R. W. (1968). Design of steel-encased concrete beam-columns. *Journal of the Structural Division*, 94, 267–282.
- Gardner, N.J., Jacobson, E.R. (1967). Structural behavior of concrete filled steel tubes, ACI Journal Proceedings. ACI.
- Giakoumelis, G., & Lam, D. (2004). Axial capacity of circular concrete-filled tube columns. *Journal of Constructional Steel Research*, 60, 1049–1068.
- Gourley, B. C., Tort, C., Denavit, M. D., Schiller, P. H., & Hajjar, J. F. (2008). *A synopsis of studies of the monotonic and cyclic behavior of concrete-filled steel tube members, connections, and frames*. Newmark Structural Engineering Laboratory: University of Illinois at Urbana-Champaign.
- Guler, S., Çopur, A., & Aydoğan, M. (2013). Axial capacity and ductility of circular UHPC-filled steel tube columns. *Magazine of Concrete Research*, 65, 898–905.
- Hamidian, M. R., Jumaat, M. Z., Alengaram, U. J., Sulong, N. R., & Shafiq, P. (2016a). Pitch spacing effect on the axial compressive behaviour of spirally reinforced concrete-filled steel tube (SRCFT). *Thin-Walled Structures*, 100, 213–223.
- Hamidian, M. R., Shafiq, P., Jumaat, M. Z., Alengaram, U. J., & Sulong, N. R. (2016b). A new sustainable composite column using an agricultural solid waste as aggregate. *Journal of Cleaner Production*, 129, 282–291.
- Han, L.-H., Li, W., & Bjorhovde, R. (2014). Developments and advanced applications of concrete-filled steel tubular (CFST) structures: members. *Journal of Constructional Steel Research*, 100, 211–228.
- Han, L.-H., Uy, B., Tao, Z., Mashiri, F., Zhu, X., Mirza, O., Tan, E.L., 2010. Some recent developments of concrete filled steel tubular (CFST) structures in China, Proceedings of the 4th international conference on steel & composite structures, pp. 43–54.
- Han, L.-H., Yao, G.-H., & Zhao, X.-L. (2005). Tests and calculations for hollow structural steel (HSS) stub columns filled with self-consolidating concrete (SCC). *Journal of Constructional Steel Research*, 61, 1241–1269.
- Hassanpour, M., Shafiq, P., & Mahmud, H. B. (2012). Lightweight aggregate concrete fiber reinforcement—a review. *Construction and Building Materials*, 37, 452–461.
- Hossain, K. M., & Chu, K. (2019). Confinement of six different concretes in CFST columns having different shapes and slenderness. *International Journal of Advanced Structural Engineering*, 11, 255–270.
- Huang, C., Yeh, Y.-K., Liu, G.-Y., Hu, H.-T., Tsai, K., Weng, Y., et al. (2002). Axial load behavior of stiffened concrete-filled steel columns. *Journal of Structural Engineering*, 128, 1222–1230.
- Jialin, T. (1996). Modeling of stress-strain relationships for steel and concrete in concrete filled circular steel tubular columns. *Kou kouzou Rombunshuu*, 3, 35–46.
- Jiaru, Q., Gang, W., Zuozhou, Z., & Zhao, K. (2004). Research on section moment-curvature relationship curves of steel tube confined high-strength concrete members. *Industrial Construction*, 34, 70–73.
- Knowles, R. B., & Park, R. (1969). Strength of concrete filled steel tubular columns. *Journal of the Structural Division*, 95, 2565–2588.
- Knowles, R. B., & Park, R. (1970). Axial load design for concrete filled steel tubes. *Journal of the Structural Division*, 96, 2125–2153.
- Kozul, R., Darwin, D., 1997. Effects of aggregate type, size, and content on concrete strength and fracture energy. University of Kansas Center for Research, Inc.
- Li, Y., Cai, C. S., Liu, Y., Chen, Y., & Liu, J. (2016). Dynamic analysis of a large span specially shaped hybrid girder bridge with concrete-filled steel tube arches. *Engineering Structures*, 106, 243–260.
- Lu, Z.-H., & Zhao, Y.-G. (2010). Suggested empirical models for the axial capacity of circular CFT stub columns. *Journal of Constructional Steel Research*, 66, 850–862.
- Matsui, C. (1994). Structural performance and design of concrete filled steel tubular structures. *Kou Kouzou Rombunshuu*, 1, 11–24. (in Japanese).
- Matsumoto, S., Komuro, T., Narihara, H., Kawamoto, S.-i., Hosozawa, O., Morita, K., 2012. Structural Design of an Ultra High-rise Building Using Concrete Filled Tubular Column with Ultra High Strength Materials, 15th World Conference on Earthquake Engineering (15 WCEE), Lisbon, Portugal.
- Nishiyama, I., & Morino, S. (2002). *Summary of research on concrete-filled structural steel tube column system carried out under the US-Japan cooperative research program on composite and hybrid structures*. Ministry of Construction: Building Research Institute.
- Park, R., Paulay, T., 1975. Reinforced concrete structures. John Wiley & Sons.
- Raizamzamani, M. M., Azerai, A., & Hanizah, A. (2019). Confinement effects on circular steel tubes filled with foamed concrete (FCFST) subjected to axial thrust and bending. *Asian Journal of Civil Engineering*, 20, 1021–1035.
- Rakhsanimehr, M., Esfahani, M. R., Kianoush, M. R., Mohammadzadeh, B. A., & Mousavi, S. R. (2014). Flexural ductility of reinforced concrete beams with lap-spliced bars. *Canadian Journal of Civil Engineering*, 41, 594–604.
- Roeder, C., Lehman, D., 2012. Initial investigation of reinforced concrete filled tubes for use in bridge foundations Washington State Transportation Center (TRAC), USA.
- Salgar, P. B., & Patil, P. S. (2019). Experimental Investigation on Behavior of High-Strength Light weight Concrete-Filled Steel Tube Strut under Axial Compression. *INAE Letters*, 4, 207–214.
- Schneider, S.P., Kramer, D.R., Sarkkinen, D.L., 2004. The design and construction of concrete-filled steel tube column frames, 13th World Conference on Earthquake Engineering, Vancouver, BC, Canada.
- Shafiq, P., Jumaat, M. Z., & Mahmud, H. (2010). Mix design and mechanical properties of oil palm shell lightweight aggregate concrete: a review. *International Journal of the Physical Sciences*, 5, 2127–2134.
- Shafiq, P., Jumaat, M. Z., & Mahmud, H. (2011a). Oil palm shell as a lightweight aggregate for production high strength lightweight concrete. *Construction and Building Materials*, 25, 1848–1853.
- Shafiq, P., Jumaat, M. Z., Mahmud, H. B., & Alengaram, U. J. (2011b). A new method of producing high strength oil palm shell lightweight concrete. *Materials and Design*, 32, 4839–4843.
- Shafiq, P., Mahmud, H. B., & Jumaat, M. Z. (2012). Oil palm shell lightweight concrete as a ductile material. *Materials and Design*, 1980–2015(36), 650–654.
- Shams, M., Saadeghvaziri, M., 1999. Nonlinear response of concrete-filled steel tubular columns under axial loading. *ACI Structural Journal* 96.
- Teo, D. C., Mannan, M. A., & Kurian, J. V. (2006a). Flexural behaviour of reinforced lightweight concrete beams made with oil palm shell (OPS). *Journal of advanced concrete technology*, 4, 459–468.
- Teo, D. C. L., Mannan, M. A., & Kurian, V. J. (2006b). Structural concrete using oil palm shell (OPS) as lightweight aggregate. *Turkish Journal of Engineering and Environmental Sciences*, 30, 251–257.
- Teo, D., Mannan, M. A., Kurian, V., & Ganapathy, C. (2007). Lightweight concrete made from oil palm shell (OPS): structural bond and durability properties. *Building and Environment*, 42, 2614–2621.

- Xiamuxi, A., & Hasegawa, A. (2012). A study on axial compressive behaviors of reinforced concrete filled tubular steel columns. *Journal of Constructional Steel Research*, 76, 144–154.
- Xiao, Y., He, W., Mao, X., Choi, K., Zhu, P., 2003. Confinement design of CFT columns for improved seismic performance, Proceeding of the Annual Conference of Japan Concrete Institute, pp. 517-530.
- Xue, J.-Q., Briseghella, B., & Chen, B.-C. (2012). Effects of debonding on circular CFST stub columns. *Journal of Constructional Steel Research*, 69, 64–76.
- Yu, Z.-W., Ding, F.-X., & Cai, C. (2007). Experimental behavior of circular concrete-filled steel tube stub columns. *Journal of Constructional Steel Research*, 63, 165–174.
- Yu, X., Tao, Z., & Song, T.-Y. (2016). Effect of different types of aggregates on the performance of concrete-filled steel tubular stub columns. *Materials and Structures*, 49, 3591–3605.

- Zeghiche, J., & Chaoui, K. (2005). An experimental behaviour of concrete-filled steel tubular columns. *Journal of Constructional Steel Research*, 61, 53–66.
- Zhang, X., Kuang, X., Yang, J., & Fan, Y. (2019). Bearing Capacity of Stone-Light-weight Aggregate Concrete-Filled Steel Tubular Stub Column Subjected to Axial Compression. *KSCE Journal of Civil Engineering*, 23, 3122–3134.

Publisher's Note

Springer Nature remains neutral with regard to jurisdictional claims in published maps and institutional affiliations.

Submit your manuscript to a SpringerOpen[®] journal and benefit from:

- ▶ Convenient online submission
- ▶ Rigorous peer review
- ▶ Open access: articles freely available online
- ▶ High visibility within the field
- ▶ Retaining the copyright to your article

Submit your next manuscript at ▶ [springeropen.com](https://www.springeropen.com)
